**Academic Journal of Science and Technology**
ISSN: 2771-3032 | Vol. 14, No. 2, 2025

# Analysis of Factors Affecting the Production Capacity of Diamond-shaped Anti-Nine-point Fracturing Well Network in Chang 8 Reservoir of Heshui Oilfield

**Liyan Zou[1, 2], Ke Wang[1, *]**

[1]School of Earth Sciences and Engineering, Xi'an Shiyou University, Xi'an 710065, China
[2]China Changqing Oilfield Branch No. 12 Oil Production Plant, China
[*]Corresponding Author: WANG Ke

**Abstract:** The Chang 8 ultra-low permeability reservoir in Heshui Oilfield has a typical "three low" characteristics. The reservoir economic development needs to use fracturing to increase the productivity of single well. Based on the theory of multiphase seepage, the author is based on the Heshui Oilfield. The seepage characteristics of the rhombohedral anti-nine-point fracturing well pattern in low-permeability reservoirs were studied in a zoning study, and an oil-water two-phase seepage model considering non-Darcy matrix seepage zone, elliptical radial flow zone and pressure crack control zone was established. The results show that in the initial stage of vertical well fracturing well pattern development, the smaller the well spacing, the higher the oil production, but the faster the water content rises. In the initial stage of small row spacing, the vertical well fracturing well spacing has little effect on the accumulated yield, but the water cut in the small row is faster. The row spacing should be optimized reasonably. The larger the crack length, the higher the yield and the water content. The faster the ascending speed is, the larger the flow capacity of the pressure crack is, the larger the accumulated capacity is. As the fracture conductivity increases, the increase of the cumulative yield becomes smaller, and the water content increases faster. The direction of the injection well and the main crack The angle of the pair is small for the output.

**Keywords:** Ultra-low permeability reservoir; diamond-shaped anti-nine-point well pattern; conductivity; crack length.

## 1. Introduction

Chang 8 reservoir of Heshui Oilfield in Ordos Basin is a typical ultra-low permeability reservoir with "low pressure, low yield and low permeability" as its typical characteristics, which needs to be transformed by hydraulic fracturing to obtain economic productivity. The Chang8 reservoir in Heshui Oilfield is a set of braided river delta deposits developed under the background of lake basin expansion and high steep slope, and the main NE30° micro-fractures are obviously developed. The average porosity of the reservoir is 10.09%, the average permeability is 0.46mD, the physical property of the reservoir is poor, the oil-water two-phase flow area is small, the bound water and the residual oil saturation are 37.33% and 34.23%, respectively, and the oil displacement efficiency is poor. The development practice of ultra-low permeability reservoir shows that the well spacing adjustment of rhomboid reverse nine-point development pattern can adapt to different types of low permeability reservoirs. However, in the rhomboid-reverse nine-point development well pattern with fracturing, the seepage law becomes complicated and the distribution of remaining oil in the well pattern changes[1-2]. Therefore, it is of guiding significance[3] to study the construction parameters of the corner well fracturing in the rhombic reverse nine-point well pattern to improve the displacement efficiency in the well pattern.

## 2. Physical Model Theory

Ultra-low permeability reservoir adopts fracturing mining mode, the seepage flow in the fracturing area is different from the conventional unmodified area, and the diamond-shaped reverse nine-point well pattern is divided into three seepage zones: the first zone is the high-speed seepage zone controlled by pressure fracture, the second zone is the elliptical seepage zone within the fracture range, and the third zone is the matrix seepage zone[4-6] far from the pressure fracture control.

## 3. Two-phase Percolation Model in The Three Zones

Assumed conditions:

(1) The oil-water phase is incompressible and the formation temperature is constant.

(2) the influence of gravity and capillary force is not considered;

(3) the reservoir is homogeneous.

Considering the symmetry characteristic of the rhomboidal inverse nine-point well pattern, the representative unit in the well pattern is selected and the seepage law of the well pattern is obtained by the superposition principle.

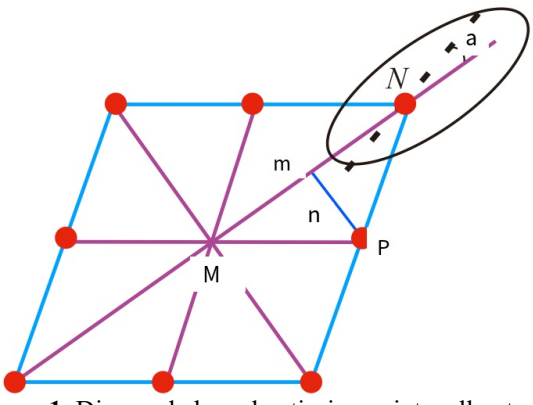


**Figure 1.** Diamond-shaped anti-nine point well network diagram

### 3.1. Zone 1: high speed seepage zone in crack

The experiment of porous media seepage mechanics shows that in Darcy flow process, as the seepage velocity increases, the linear relationship between it and pressure gradient will not exist. In the transition zone, it is called "nonlinear seepage", and there are two kinds of resistance, namely viscous force and inertial force.[7-10]

$$\frac{dp}{dx} = -\left(\frac{\mu}{k}v + \beta\rho v^2\right) \tag{1}$$

Where, $p$ is the oil reservoir pressure, MPa; $\mu$ is fluid viscosity, mpa·s; k is reservoir permeability, mD; $v$ fluid flow velocity, m/s; $\beta$ is the nonlinear flow coefficient; $\rho$ is the fluid density g/cm³.

### 3.2. Zone 2: Elliptical seepage in the crack range

Within the control range of pressure fracture transformation, the pressure wave is transmitted in an almost ellipsoidal way, and the flow in zone 2 is ellipsoidal seepage. Based on the concept of ellipsoidal percolation, the varying rectangular cluster is used to describe the isobaric elliptic cluster[11-13].

$$\begin{aligned} \bar{x} &= x_{\mathrm{f}} \cosh\xi \ , \\ \bar{y} &= \frac{2}{\pi}\int_0^{2\pi} n\sin\eta d\eta = \frac{2x_{\mathrm{f}}}{\pi}\sinh\xi \end{aligned} \tag{2}$$

Where: $x_{\mathrm{f}}$ is the length of pressure crack, m; n is the row distance, m.

Then the partial differential equation of the seepage flow of the ellipse in the second zone is:

$$\frac{\partial}{\partial y}\left[\frac{kk_{ro}}{\mu_o}\left(\frac{\partial p}{\partial y} - G\right)\right] = \phi\frac{\partial S_o}{\partial t} \tag{3}$$

$$\frac{\partial}{\partial y}\left[\frac{kk_{rw}}{\mu_w}\left(\frac{\partial p}{\partial y} - G\right)\right] = \phi\frac{\partial(1-S_o)}{\partial t} \tag{4}$$

Where: $k_{\mathrm{ro}}$ is the relative permeability of oil phase; $k_{\mathrm{rw}}$ is the water phase relative permeability; $G$ is the starting pressure gradient, Mpa/m; $S_{\mathrm{o}}$ is oil saturation; $\mu_{\mathrm{o}}$ is the oil phase viscosity, mpa·s; $\mu_{\mathrm{w}}$ is the oil phase viscosity, mpa·s.

The flow rate formula is:

$$Q = 8x_{\mathrm{f}}^2\sinh\xi\cos\xi\left[\frac{kk_{rw}}{\mu_w}\left(\frac{\partial p}{\partial y} - G\right)\right] \tag{5}$$

Where: $\xi$ is the outer boundary of the ellipse.

The elliptic flow rate in the well pattern unit area is a part of the elliptic seepage flow, namely:

$$m = \frac{Q_t}{Q} = \frac{M_t}{M} \tag{6}$$

Where: $M_{\mathrm{t}}$ is the area of the ellipse falling in the well pattern unit area; $Q_{\mathrm{t}}$ is the elliptic flow rate in the well pattern unit area; $M$ is the area of the ellipse.

The corner well on the long diagonal in the rhomboid anti-nine-point pattern unit, where m is

$$m = ar\cos\left(3l_m / \sqrt{9l_m^2 + 4l_n^2}\right)/\pi \tag{7}$$

Short diagonal corner Wells are:

$$m = ar\cos\left(6l_n / \sqrt{9l_m^2 + 36l_n^2}\right)/\pi \tag{8}$$

Side well on the long diagonal:

$$m = ar\cos\left(l_m / \sqrt{l_m^2 + 4l_n^2} - \alpha\right)/\pi \tag{9}$$

Side well on the short diagonal:

$$m = ar\cos\left(4l_n / \sqrt{l_m^2 + 4l_n^2} - \alpha\right)/\pi \tag{10}$$

### 3.3. Zone 3: Far away from the pressure fracture control matrix seepage zone

The fluid flow in the third zone is the plane radial non-Darcy flow law, which is simplified to the relationship[14-17] between the independent variables $r$ and t. The partial differential equation of percolation can be written as:

$$\frac{\partial}{\partial r}\left[-\frac{kk_{ro}}{\mu_o}\left(\frac{\partial p}{\partial r} - \lambda\right)\right] + q_o = \phi\frac{\partial S_o}{\partial t} \tag{11}$$

$$\frac{\partial}{\partial r}\left[-\frac{kk_{rw}}{\mu_w}\left(\frac{\partial p}{\partial r} - \lambda\right)\right] + q_w = \phi\frac{\partial(1-S_o)}{\partial t} \tag{12}$$

Where: q is the source and sink term, which can be written as:

$$q_o = \frac{q}{ah}[1 - f_w]\delta(x - x_m)\delta(y - y_m) \tag{13}$$

$$q_w = \frac{q_{\mathrm{l}}}{bh}[1 - f_w]\delta(x - x_n)\delta(y - y_n) \tag{14}$$

Where: q and $q_{\mathrm{l}}$ are the flow rate of injection well and production well respectively, δ is the Dirac function, f is the *water*$_{\mathrm{w}}$ *cut*, %. Considering that the flow rate of the injection well and the production well is only a part of the flow rate of the well, according to the flow line distribution, the flow rate in the flow line control area should be divided by the corresponding coefficients a and b, for the diamond-shaped inverse nine-point well pattern, a=8, b=16.

### 3.4. Condition of definite solution

Initial conditions

$$\begin{cases} p(r = r_w, t = 0) = p_o \\ p(r = l_a, t = 0) = p_w \\ s_w(\xi, 0) = s_{wc} \end{cases} \tag{15}$$

Where: $p_o$ is the bottom hole flow pressure of the oil well, MPa; $p_w$ is the bottom-hole flow pressure of the well, MPa; $r_w$ is wellbore radius, m; $s_{wc}$ is the original water saturation, %.

The inner boundary conditions are

$$r\frac{\partial p_o}{\partial r}\bigg|_{r=r_w} = \frac{q_o\mu}{2\pi Kh} \tag{16}$$

$$r\frac{\partial p_w}{\partial r}\bigg|_{r=r_w} = \frac{q_w\mu}{2\pi Kh} \tag{17}$$

The outer boundary conditions are:

$$\frac{\partial p}{\partial n}\bigg|_C = 0 \tag{18}$$

The interface conditions for Zone 2 and Zone 3 are:

$$p_1 = p_2\big|x_f \to \xi_0,\ \ p_2 = p_3\big|_{r=\xi} \tag{19}$$

In the formula:, M, N are respectively the short and short semi-axes of the ellipse,, and are the inner boundaries of the ellipse. $r = \sqrt{M^2\cos^2\alpha + N^2\sin^2\alpha}$ $M = x_f\cosh\xi$ $N = x_f\sinh\xi$ $\xi_0$

### 3.5. Reservoir matrix-fracture coupling flow equation

$$p_w - p_o - G(r-r_o) - \frac{2x_fG}{\pi}[\sinh\xi - \sinh\xi_0] = \frac{\mu}{k_f}\frac{qx_f}{w_fh} + \int_0^{x_f}\xi\rho\left(\frac{q}{w_fh}\right)^2 dx + \frac{\alpha q\mu_o}{4\pi kx_f}\cdot\int_{\xi_0}^{\xi}\frac{q}{\sinh\xi\left(\frac{k_{rw}}{\mu_w}+\frac{k_{ro}}{\mu_0}\right)}d\xi + \frac{q}{bk\phi n^2}\cdot\int_0^t\frac{q_I}{c}dt\int_{s_{w0}}^{s_{wf}}\frac{f_w''}{\sinh\xi\left(\frac{k_{rw}}{\mu_w}+\frac{k_{ro}}{\mu_0}\right)}ds_w \tag{20}$$

## 4. Analysis of Influencing Factors of Fracturing

Data of rhomboid-reverse nine-point development zone of an ultra-low permeability reservoir in Ordos Basin: Well spacing is 540m, row spacing is 130m, reservoir depth is 1834m, effective oil thickness is 16.0m, average porosity is 0.11, oil saturation is 0.45, average oil permeability is 0.70mD, injection and production pressure difference is 13.6MPa, fracture half-length is 96m, fracture conductivity is 0.2μm²·m, fracture width is 0.002m.

### 4.1. Diamond inverse nine-spot well spacing

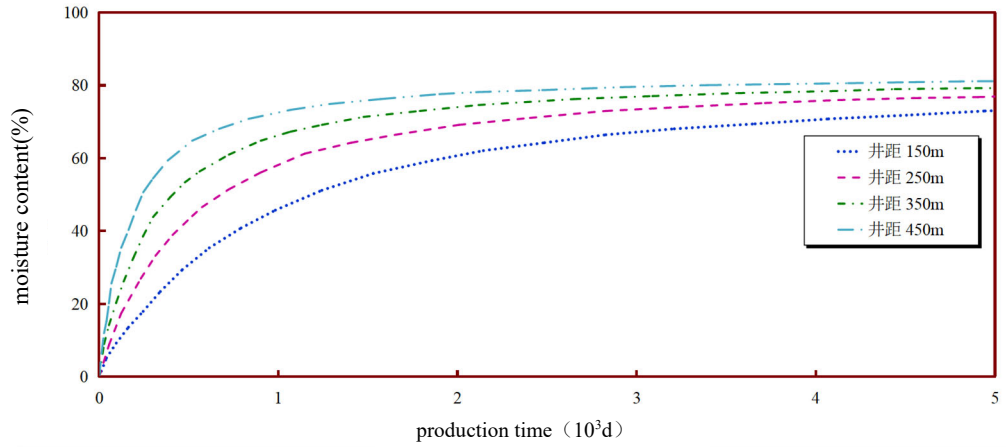


(2a)

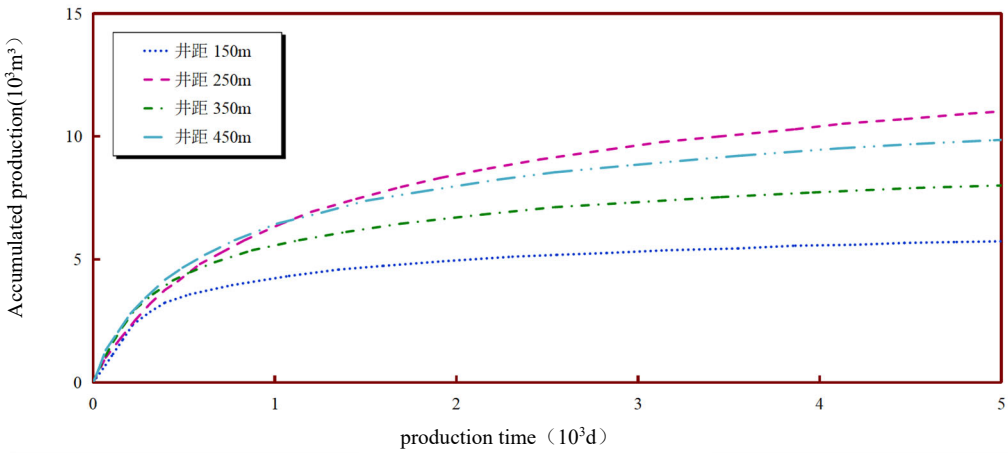


(2b)

**Figure 2.** The relationship between yield and water content of different well spacings with time

As can be seen from FIG. 2, the smaller the well spacing of vertical well fracturing pattern in the early stage of development, the higher the cumulative oil production, but the greater the increase of water cut. The water cut growth rate of the inverted nine points of the diamond well spacing is lower, and its cumulative oil production exceeds that of the small well spacing near 800 days.

## 4.2. Rhomboid reverse nine-point spacing

As can be seen from FIG. 3, in the early stage of development, vertical well fracturing pattern spacing has little influence on cumulative production, but water cut increases faster in small row spacing. At around 1600d, the cumulative production of different row spacing increased slightly and basically approached a straight line.

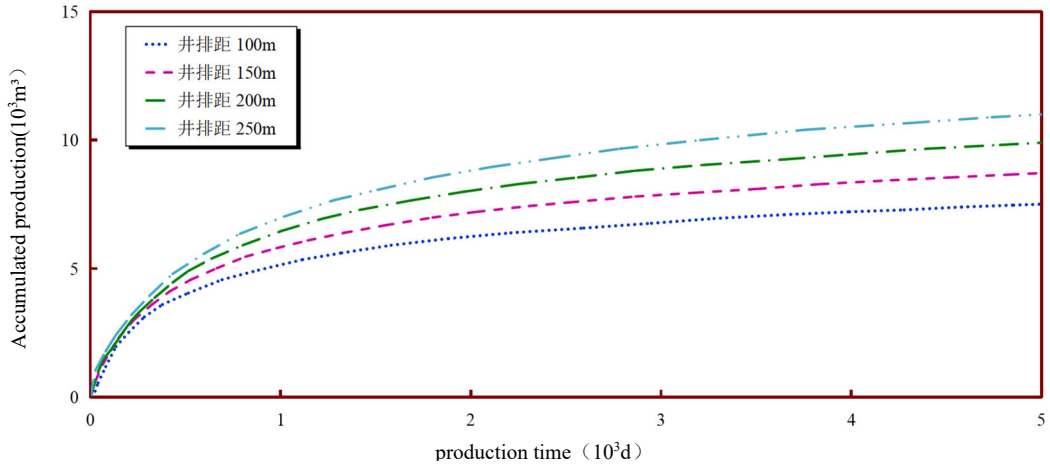


(3a)

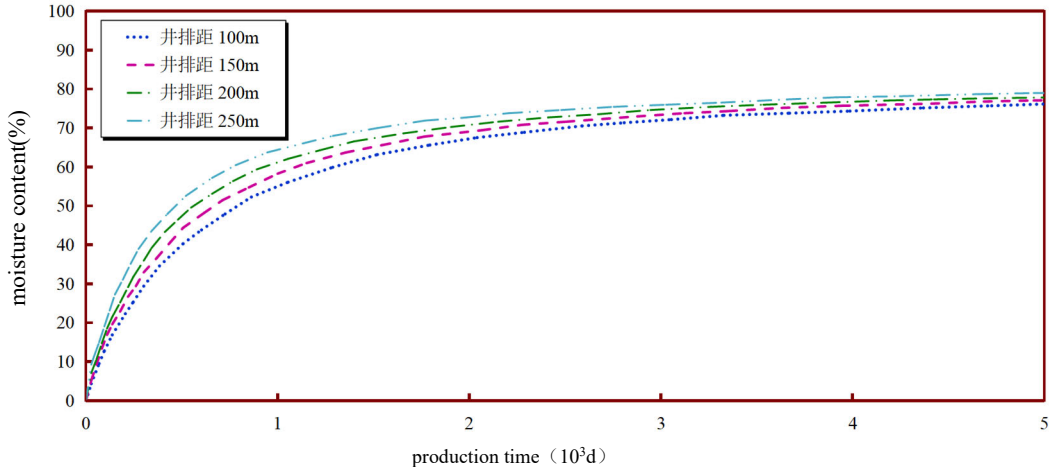


(3b)

**Figure 3.** The relationship between different row spacing yield and water content with time

## 4.3. Press the crack half length

As can be seen from FIG. 4, the cumulative production increases rapidly within 800d, and the corresponding water content changes rapidly from 0 to 50%. The main production period of ultra-low permeability reservoir is concentrated in the middle and low water cut section. The longer the fracture, the higher the production, but the faster the water cut rises.

## 4.4. Pressure crack conductivity

As can be seen from Figure 5, the greater the conductivity of pressure fractures in vertical Wells, the higher the cumulative oil production and the greater the increase in water content. It can be seen that the validity period of fracturing well pattern development is concentrated in the early and middle stages of development.

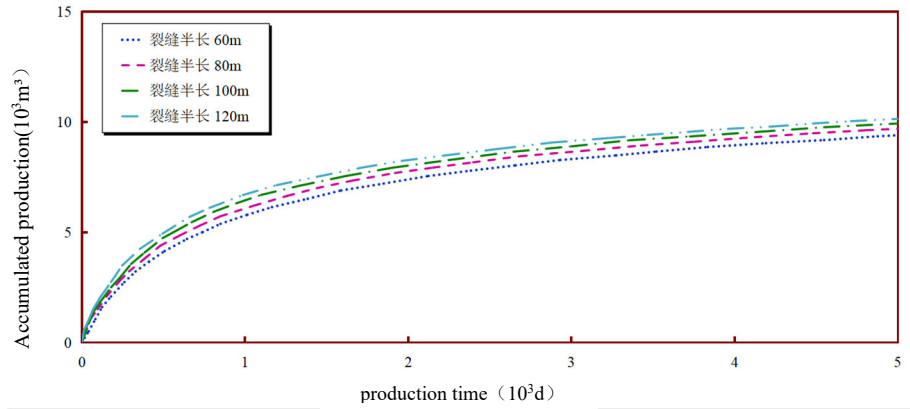


(4a)

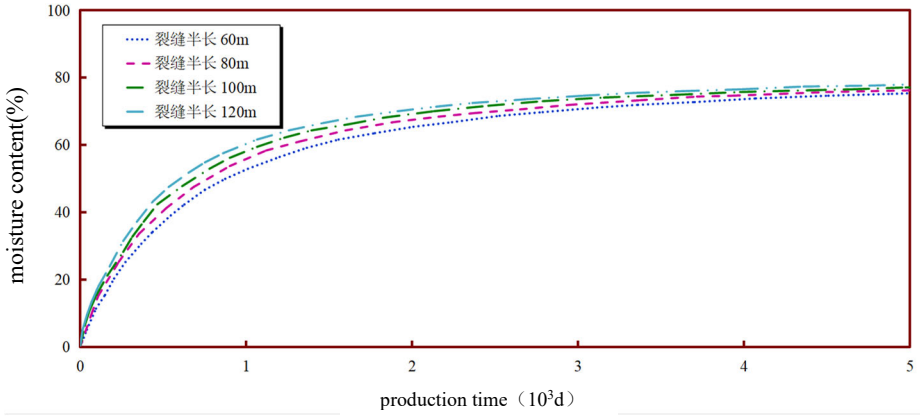


(4b)

**Figure 4.** The relationship between half-length yield and water content of different cracks with time

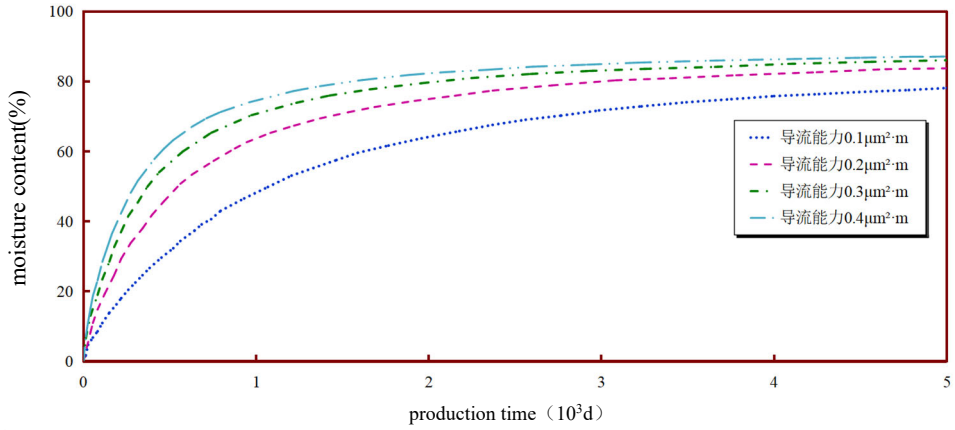


(5a)

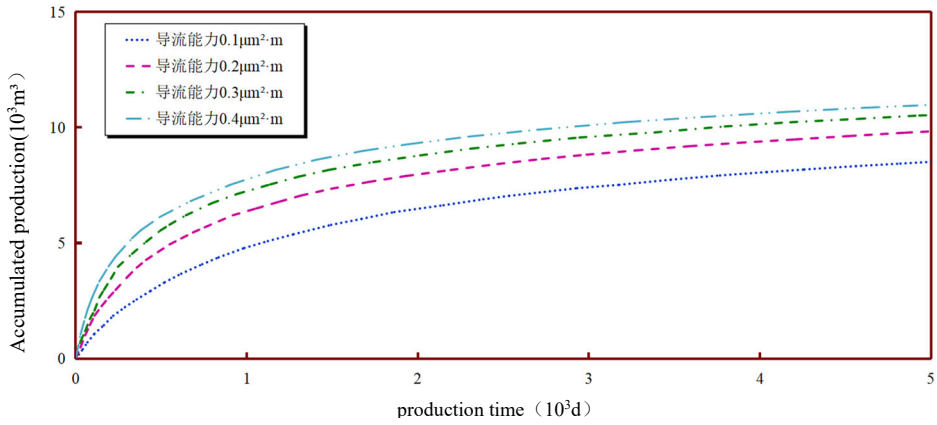


(5b)

**Figure 5.** The relationship between yield and water content of different fracture conductivity

### 4.5. Angle between the connecting direction of the well and the main fracture

As can be seen from Figure 6, for the same water content of Angle Wells, the smaller the Angle, the higher the cumulative production. With the increase of water cut, under the same water cut, the greater the Angle, the higher the degree of production. On the whole, the Angle between the connection direction of water injection well and the main fracture has little effect on production.

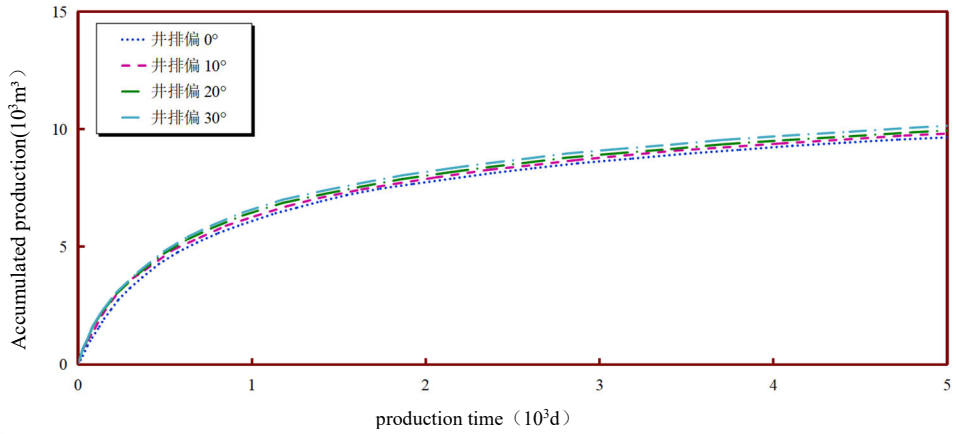


(6a)

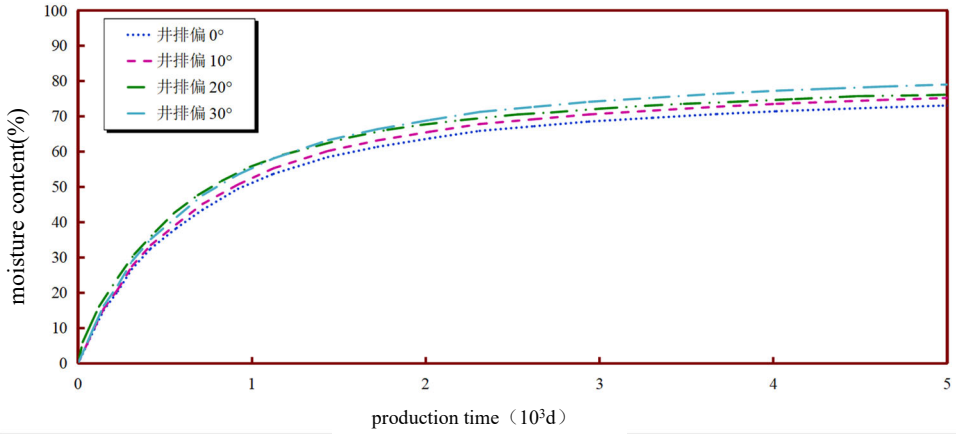


(6b)

**Figure 6.** The relationship between yield and water content with time under different fracture conductivity

## 5. Conclusion

(1) Based on the theoretical characteristics of percolation, the characteristics of percolation in the rdiamond-shaped reverse nine-point fracturing pattern were studied in different zones, and a three-zone two-phase fracturing model was established considering the matrix non-Darcy percolation, elliptical radial flow and linear fracture flow of starting pressure gradient.

(2) In the initial stage of small row spacing, the vertical fracturing pattern row spacing has little influence on the cumulative production, but the water cut rising rate of small row spacing is faster, so the row spacing should be optimized reasonably; The larger the fracture length, the higher the cumulative production and the faster the water cut increase; The smaller the fracture conductivity, the lower the cumulative yield. With the increase of fracture conductivity, the increase of cumulative yield becomes smaller, and the increase of water content is faster. The Angle between the connection direction of water injection well and the main fracture has little effect on the production.

## References


[1] WANG Ming, ZHU Wei-yao, LI Ji-shan, et al. Two-phase seepage analysis of rhombohedral nine-point fracturing well pattern in low permeability reservoir[J]. Rock and Soil Mechanics, 2010, 31(10):3295-3299.

[2] Zhu Shengju, Zhu Jie, An Xiaoping, et al. Study on the area and sweep coefficient of diamond-shaped anti-nine-point well network in low permeability reservoirs[J]. Journal of Chongqing University of Science and Technology (Natural Science Edition), 2013, 15(2): 80- 84.

[3] LIU Feng, CHEN Xiaofan. Study on Reasonable Well Spacing of Diamond-shaped Anti-Nine-point Well Pattern in Anisotropic Reservoir[J]. Journal of Southwest Petroleum University (Journal of Natural Sciences), 2016, 38(6): 125-130.

[4] He Ying. Research on reservoir engineering method for low permeability reservoir network deployment[D]. Graduate School of Chinese Academy of Sciences (Institute of Fluid Flow Mechanics), 2009.

[5] Wang Kun, Zhang Liehui. Calculation of relative permeability of oil and water in stress-sensitive ultra-low permeability reservoirs[J]. Journal of Oil and Gas Technology, 2011, 33(11): 117-119.

[6] Zhou Sibin, Qu Jianshan, Zhang Shuqin. Influence of water injection timing on development of ultra-low permeability reservoirs[J]. Fault Block Oil and Gas Field, 2008, 15(1): 63-65.

[7] LIU Hui, HE Shun-li, LI Jun-jian, et al. Study on evaluation method of water flooding development effect in ultra-low permeability reservoirs[J]. Journal of Southwest Petroleum University (Journal of Natural Sciences), 2009, 31(1): 58-60.

[8] Wang Jing, Liu Huiqing, Liu Renjing, et al. Numerical simulation of low permeability and ultra-low permeability reservoirs considering starting pressure and stress sensitivity effects[J]. Chinese Journal of Rock Mechanics and Engineering, 2013(s2): 003317-3327.

[9] Yonakang Fu. Current Status of Research on Graphene-reinforced Titanium Matrix Composites[J].Academic Journal of Science and Technology,2025,14(1):1-11

[10] Rui Guo.A Review of Methods for Studying Reservoir Heterogeneity [J]. Academic Journal of Science and Technology, 2025, 14(1):145-149

[11] Boru Meng. Exploration of Charging Technology for New Energy Electric Vehicles[J].Academic Journal of Science and Technology, 2025, 14(1): 101-106

[12] Hao Ding, Xiaoziyu Fang. Tudy on Urban Waterfront Space Renewal from the Perspective of Residents' Health [J]. Academic Journal of Science and Technology, 2025, 14(1): 107-112.